APPLIED AND ENVIRONMENTAL MICROBIOLOGY, Apr. 1982, p. 924-938
0099-2240/82/040924-15$02.00/0

Vol. 43, No. 4

Iron Oxidation and Precipitation of Ferric Hydroxysulfates by Resting *Thiobacillus ferrooxidans* Cells

NORMAN LAZAROFF,* WARREN SIGAL, AND ANDREW WASSERMAN

Department of Biological Sciences, State University of New York at Binghamton, Binghamton, New York 13901

Received 5 October 1981/Accepted 5 January 1982

The oxidation of ferrous ions, in acid solution, by resting suspensions of *Thiobacillus ferrooxidans* produced sediments consisting of crystalline jarosites, amorphous ferric hydroxysulfates, or both. These products differed conspicuously in chemical composition and infrared spectra from precipitates formed by abiotic oxidation under similar conditions. The amorphous sediments, produced by bacterial oxidation, exhibited a distinctive fibroporous microstructure when examined by scanning electron microscopy. Infrared spectra indicated outer-sphere coordination of Fe(III) by sulfate ions, as well as inner-sphere coordination by water molecules and bridging hydroxo groups. In the presence of excess sulfate and appropriate monovalent cations, jarosites, instead of amorphous ferric hydroxysulfates, precipitated from bacterially oxidized iron solutions. It is proposed that the jarositic precipitates result from the conversion of outer-sphere (T_d) sulfate, present in a soluble polymeric Fe(III) complex, to inner-sphere (C_{3v}) bridging sulfate. The amorphous precipitates result from the further polymerization of hydroxo-linked iron octahedra and charge stabilized aggregation of the resulting iron complexes in solution. This view was supported by observations that bacterially oxidized iron solutions gave rise to either amorphous or jarositic sediments in response to ionic environments imposed after oxidation had been completed and the bacteria had been removed by filtration.

An important but poorly understood feature of chemolithotrophic iron oxidation by *Thiobacillus ferrooxidans* is its requirement for sulfate ions (9, 18, 24). Although the requirement is partially spared by anions such as phosphate, arsenate, tungstate, or tellurate, only selenate can completely substitute for sulfate in supporting Fe^{2+} oxidation by resting cell suspensions (10). This requirement for sulfate in iron oxidation is reflected in the composition of the iron sediments deposited by the iron-oxidizing thiobacilli in nature and in laboratory cultures (3, 11, 23). Ivarson (6) demonstrated that the iron sediments produced by *T. ferrooxidans* contained ferric hydroxysulfates identical to naturally occurring jarosites of composition $MFe_3(SO_4)_2(OH)_6$, where M is one of several cations, including H_3O^+, Na^+, K^+, and NH_4^+.

Ivarson's work suggested a causal relationship between the widespread occurrence of jarosites in nature and the chemical activities of organisms like *T. ferrooxidans*, which oxidize and leach pyritic substrates. Consequently, the realization that sulfate is required for iron oxidation led us to consider whether the precipitation of ferric hydroxysulfates by bacterial action involved iron sulfate complexes of particular significance to the chemolithotrophic iron metabolism of *T. ferrooxidans*.

In pursuing this question, we compared the infrared (IR) spectra of iron precipitates formed by resting cell suspensions of *T. ferrooxidans* with spectra of oxidized iron precipitates formed abiotically and examined the effects of ionic composition on the nature of the precipitates formed. From our perspective, it was of particular interest to learn whether jarosites were inevitably formed as insoluble products of bacterial iron oxidation or whether other products resulted if the ionic environment was altered.

MATERIALS AND METHODS

The Leathen strain of *T. ferrooxidans* was propagated in 10 liters of aerated 9K medium of Silverman and Lundgren (20). Cells were then harvested and washed by centrifugation as described previously (22).

The formation of bacterially oxidized iron precipitates was carried out in 100-ml volumes of solution containing 0.1 to 0.2 M Fe^{2+}, adjusted to pH 2.5 with H_2SO_4, and dispensed in cotton-plugged 250-ml Erlenmeyer flasks. Each flask received approximately 10^{11} cells of *T. ferrooxidans* suspended in H_2SO_4, pH 2.5. The flasks were then incubated, with vigorous shaking on a rotary shaker, for 10 days at room temperature. Under such conditions bacteria do not grow, even though the ferrous ions may be nearly completely oxidized by the end of the incubation period (Table 1).

Iron precipitates were similarly recovered from bac-

TABLE 1. Formation and characteristics of two types of iron precipitates produced by resting cells of *T. ferrooxidans* in ferrous sulfate solutions

Substrate[a]	% of bacteria remaining[b]	% of Fe oxidized	% of Fe precipitated	Color[c]	Sediment characteristics					
					Solubility[d]	% Fe	Fe/SO_4^{2-}	IR	% Na	Li
0.2 M $FeSO_4$	17.5	92.9	24.9	Red-brown	Sol (20°C)	53.4	4.60	Amorphous		
0.2 M $FeSO_4$ + 0.2 M Li_2SO_4	22.0	53.3	7.4	Light red-brown	Sol (20°C)	55.5	4.42	Amorphous		ND[e]
0.2 M $FeSO_4$ + 0.2 M $NaClO_4$	47.5	21.2	6.4	Pale yellow	Insol (20°C) Sol (55°C)	36.6	1.55	Jarosite	3.5	
0.2 M $FeSO_4$ + Li_2SO_4 + $NaClO_4$	42.5	18.5	6.4	Yellow	Insol (20°C) Sol (55°C)	34.5	1.44	Jarosite	3.75	ND

[a] 100 ml, pH 2.5; inoculated with 10^{11} cells and incubated in shaken 250-ml Erlenmeyer flasks at 23°C for 2 weeks.
[b] Percentage of initial direct microscopic count of bacterial cells after 2 weeks of incubation.
[c] Color of dried sediment.
[d] In 4 N HCl. Sol, soluble; insol, insoluble.
[e] ND, Not detectable.

terially oxidized ferrous sulfate solutions which had been filtered through 0.45-μm membrane filters to remove bacteria before completion of ferric hydroxysulfate precipitation. Treatment by addition of metal salts was compared with control treatments, without additions, to study the effects of the ionic environment on the nature of the precipitates formed.

Abiotically oxidized iron precipitates were obtained from ferrous sulfate solutions (in the presence or absence of other inorganic ions) in one of three ways: by the addition of appropriate amounts of 0.5 M H_2O_2 at pH 2.5; by spontaneous oxidation for a 3-week period in shaken flasks at pH 6.0; or by spontaneous oxidation in shaken flasks at pH 9.0 (Table 2). The iron precipitates from all preparations were recovered by centrifugation, washed twice in pH 2.5 H_2SO_4 and twice in distilled water, and then washed with acetone and dried in a forced draft oven at 80°C.

IR spectra of the iron precipitates were determined from samples incorporated in KBr disks by standard techniques and then scanned with a Beckman Acculab 6 IR spectrophotometer. Analyses for iron, sulfate, sodium, potassium, or nitrogen were carried out after weighed samples of the sediments were dissolved in 4 N HCl.

To determine iron content, we measured Fe^{3+} absorbance at 304 nm, in the presence of excess sulfate (0.4 M), according to the technique described by Steiner and Lazaroff (22). The determinations were made after dilution of 4 N HCl solutions of the iron precipitates to the range of 0.5×10^{-4} to 5.0×10^{-4} M Fe^{3+} and a chloride concentration of 0.01 M. Applicable extinction coefficients at 304 nm were first determined for solutions of increasing $[SO_4^{2-}]/[Fe^{3+}]$ in the presence of 0.01 N HCl. From these data, plots of absorbance versus Fe^{3+} were used to convert absorbance measurements to Fe^{3+} concentrations. Sulfate was determined in the hydrochloric acid solutions of the precipitates, after neutralizing with ammonium hydroxide and heating to precipitate the iron, as ferric hydroxide, before its separation by filtration. The filtrate and distilled water washings of the ferric hydroxide sediment were then combined and acidified with hydrochloric acid, and the sulfate was precipitated from hot solution by the addition of excess $BaCl_2$. The $BaSO_4$ was recovered, dried, and weighed on tared membrane filters by standard techniques.

Sodium and potassium were determined with an IL model 143 flame photometer after dilution of the acid solutions of the iron precipitates to 0.4 N HCl or less. Nitrogen was determined in the HCl solutions by the spectrophotometric micro-Nesslerization technique of

TABLE 2. Composition of abiotic iron precipitates produced by the oxidation of 0.2 M ferrous sulfate solutions

Test solution[a]	% Fe	Fe/SO_4^{2-}
pH 9.0 (spontaneous)		
No addition	62.72	99.12
+ 0.2 M Na_2SO_4	61.95	95.86
+ 0.2 M K_2SO_4	63.58	78.95
Avg	62.75	91.31
pH 6.0 (spontaneous)		
No addition	59.69	19.05
+ 0.2 M $(NH_4)_2SO_4$	59.84	14.10
+ 0.2 M Na_2SO_4	59.76	20.54
+ 0.2 M K_2SO_4	57.88	15.91
Avg	59.29	17.40
pH 2.5 (H_2O_2)		
No addition	51.09	6.05
+ 0.2 M $(NH_4)_2SO_4$	60.82	8.17
+ 0.2 M Na_2SO_4	49.20	3.51
Avg	53.70	5.91

[a] The pH was adjusted by addition of H_2SO_4 or NaOH.

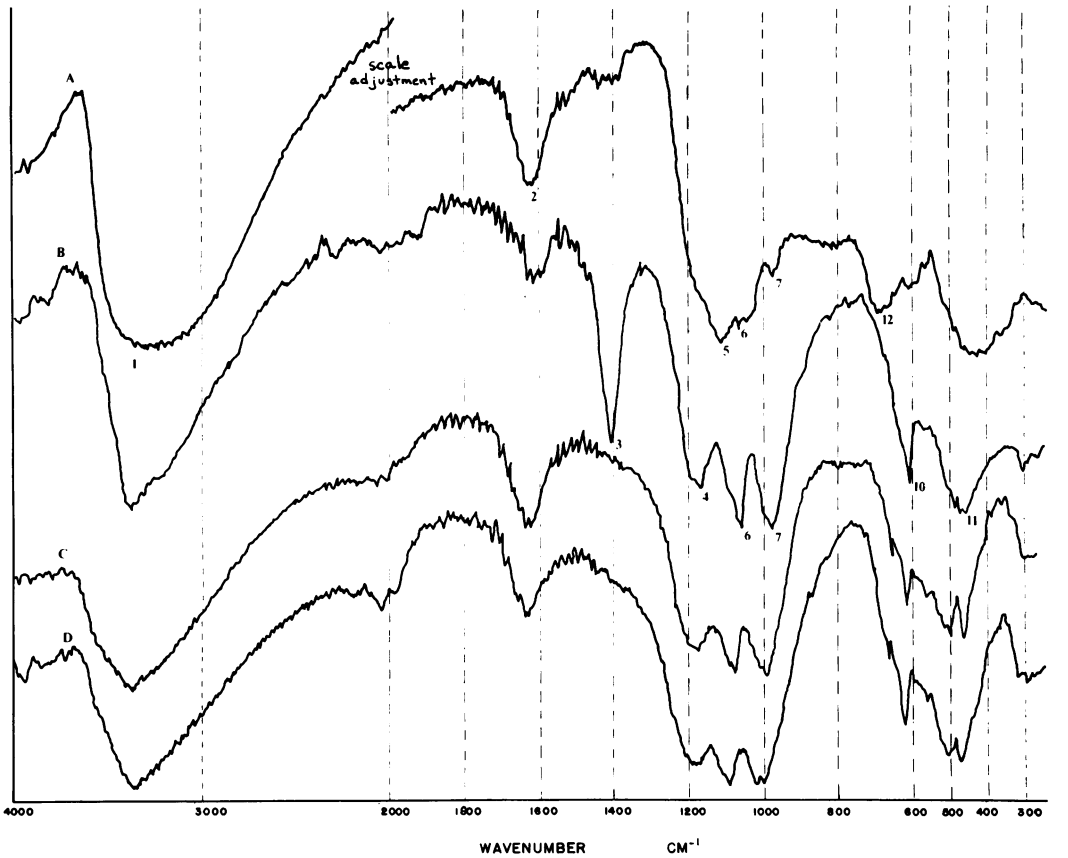

FIG. 1. IR spectra of precipitates produced in 0.2 M $FeSO_4$ solutions oxidized by *T. ferrooxidans* (pH 2.5). (A) No additions; (B) plus 0.2 M $(NH_4)_2SO_4$; (C) plus 0.2 M Na_2SO_4; (D) plus 0.2 M K_2SO_4; (1) OH stretch, (and NH stretch shoulder in B); (2) Water deformation; (3) NH_4^+ deformation; (4) $\nu_3(C_{3v})$ (SO_4^{2-}); (5) $\nu_3(T_d)$ (SO_4^{2-}); (6) $\nu_3(C_{3v})$ (SO_4^{2-}); (7) $\nu_1(SO_4^{2-})$ [and δ(OH) in B, C, and D]; (10) $\nu_4(SO_4^{2-})$; (11) τ(OH); (12) unassigned characteristic of amorphous basic iron sulfates.

Johnson (8), modified by adding sufficient sodium hydroxide to compensate for the acidity of the sample and using standards made up in dilute hydrochloric acid solutions.

RESULTS

Two types of ferric hydroxysulfate precipitates were obtained from acid ferrous sulfate solutions after bacterial oxidation. Jarosites were produced by bacterial oxidation in $FeSO_4$ solutions containing suitable monovalent cations, such as Na^+, K^+, or NH_4^+, and an excess of sulfate anions at pH 2.5. Without appropriate cations, even if excess sulfate was supplied in the form of Li_2SO_4 or $MgSO_4$, amorphous precipitates were produced. Neither the amorphous or jarositic product was formed if the same solutions were oxidized chemically under the same conditions. The most distinctive IR absorbance frequencies of jarosites (Fig. 1; Table 3) were the ν_3 mode of SO_4^{2-} at 1,180 to 1,190 and 1,070 to 1,089 cm^{-1}, δ (OH) at 984 to 1,000 cm^{-1}, and the ν_4 mode of SO_4^{2-} at 619 to 622 cm^{-1}. In addition, the jarosites displayed IR frequencies due to OH stretch at 3,350 to 3,400 cm^{-1}; the ν_1 mode of SO_4^{2-} at 1,004 to 1,017 cm^{-1} [distinguishable from δ (OH) only in some specimens]; the ν_4 mode of SO_4^{2-}, as a shoulder at 640 to 650 cm^{-1}; τ modes of OH at 487 to 510 and 465 to 480 cm^{-1}; and the ν_2 mode of SO_4^{2-} at 440 cm^{-1}. In a few preparations, $\tau(SO_4^{2-})$ frequencies of ≈350 and 312 cm^{-1} were observed as well. Even after prolonged drying of acetone-washed samples under vacuum at 80 to 100°C, most jarosite spectra possessed the water deformation at 1,620 to 1,639 cm^{-1} and absorbance at 570 cm^{-1}, ascribed to coordinated water (15). The ammonio-jarosites displayed strong absorbance due to NH_4^+ deformation at 1,416 to 1,423 cm^{-1} and NH stretch at ≈3,200 cm^{-1} as a shoulder contiguous with the OH stretching frequency.

The other type of precipitate formed by bacterial oxidation exhibited IR spectra with broad absorbance bands of the type usually associated with amorphous solids (Fig. 1A; Table 3). The spectra resembled those described by Margulis et al. (13) for an amorphous basic ferric sulfate, considered by them to be a hydrate of Fe(III) oxide sulfate. Scanning electron micrographs of the amorphous precipitates were clearly distinguishable by their fibroporous microstructure from the crystalline jarosites (Fig. 2 and 3). The amorphous-type precipitates exhibited broad bands in the OH stretching region with maxima between 3,270 and 3,340 cm^{-1}, as well as strong absorbance due to the water deformation between 1,619 and 1,630 cm^{-1}. The most distinctive IR absorbance characteristics of the amorphous precipitates were the broad bands between 1,110 and 1,120 cm^{-1}, associated with a weaker band around 970 to 978 cm^{-1}. Those features are in close agreement with the assignments for ν_3 and ν_1, respectively, of SO_4^{2-} in the outer coordination sphere of transition metal ion complexes (14, 15).

The bacterial precipitates obtained were rarely purely amorphous or purely jarositic in character. Consequently, their IR spectra were usually compounds of the two types. However, we found that the amorphous material was more soluble in 4 N HCl at room temperature than the jarosites, enabling comparison of spectra before and after washing with the hydrochloric acid as a means of distinguishing the IR spectral characteristics unique to each type. By this procedure, it became more evident that the band at $\simeq$1,115 cm^{-1} of the amorphous sediments was indeed its $\nu_3(SO_4^{2-})$ frequency, and the band at $\simeq$970 to 975 cm^{-1} was $\nu_1(SO_4^{2-})$, as described above. The shoulders and inflections in the regions of 1,170 to 1,180 and 1,070 to 1,090 cm^{-1} could be attributed to $\nu_3(SO_4^{2-})$ of jarosite present in the heterogeneous specimens (Fig. 4). The heterogeneity was confirmed in scanning electron micrographs which showed jarositic crystals in the fibrous matrix of the amorphous iron sediment (Fig. 5).

It has not been possible to assign unequivocally a frequency for OH^- deformation in the amorphous species. However, the IR absorbance between 1,040 and 1,050 cm^{-1} cannot be accounted for solely by admixture of jarosite. That this is due to the Fe-O bending mode of coordinated OH^- groups is supported by IR analysis of amorphous precipitates prepared by bacterial oxidation of iron in solutions containing sodium selenate. The selenate bands were, as expected, found at much lower frequencies than sulfate (Fig. 6). IR spectra of ferric selenate reported in the literature (16) and our preparations show that $T_d(SeO_4^{2-})$ has a ν_3 band at $\simeq$870 cm^{-1}. In the partly selenated analog, the absorbance maximum at 1,115 cm^{-1} had virtually disappeared, confirming its origin as the SO_4^{2-} group, whereas a strong absorption band remained at 1,045 cm^{-1}, suggesting that this was due to OH^- (Fig. 1).

$FeSO_4$ solutions oxidized spontaneously in shaken flasks at 23°C and pH 6.0, or with H_2O_2 at pH 2.5, yielded precipitates possessing strong IR absorption bands at $\simeq$790 and 880 cm^{-1} (Fig. 7 and 8) which appeared identical to the frequencies assigned to the δ(OH) of αFeOOH (goethite) by Shokarev et al. (19). Both preparations had broad absorbance due to water deformation. The precipitates prepared by oxidation at pH 2.5 with H_2O_2 showed greater IR-absorbing activity in the SO_4^{2-} regions of the spectrum (particularly 1,115 to 1,120 cm^{-1}) than did the precipitates prepared by spontaneous oxidation at pH 6.0. In agreement with the spectra, the H_2O_2-oxidized materials were found to have much lower iron-to-sulfur ratios than did the products of spontaneous oxidation at pH 6.0. Precipitates formed from 0.6 M $FeSO_4$, pH 1.5, oxidized slowly at room temperature over a 3-year period resembled the pH 6.0 and the H_2O_2-oxidized sediments, but with even stronger absorbance at 790 and 880 cm^{-1}. Thus, all of the sediments formed abiotically, at high or low pH and at room temperature, were distinctly different in chemical functional groups than were those formed as the result of bacterial oxidation.

Very little sulfate was present in sediments formed by spontaneous oxidation at pH 9.0 (Table 2). The latter were dark brown to black and showed virtually no absorbance in the SO_4^{2-} region of the IR spectrum; there was only slight indication of the presence of OH groups. Absorbance in the 575 cm^{-1} region (Fig. 8) and ferromagnetic properties suggested that this product was predominantly Fe_3O_4 (magnetite) (16), although other possibilities are not excluded.

Ferrous sulfate solutions supplemented with sodium, potassium, or ammonium sulfates, and oxidized by suspensions of iron bacteria, produced jarositic precipitates in which the incorporation of the monovalent cations was demonstrated by chemical analysis (Table 4). The incorporation of NH_4^+ was conveniently observed in the IR spectra of jarositic sediments derived from $FeSO_4$ solutions containing added $(NH_4)_2SO_4$, since the presence of the NH_4^+ cation produces a sharp band due to NH stretch at $\simeq$1,420 cm^{-1}. IR analyses made it evident that NH_4^+ incorporation was limited to the jarositic precipitates (Fig. 7) and did not occur in amorphous bacterial sediments or in the deposits formed by abiotic oxidation.

Clearly, the presence of appropriate monova-

TABLE 3. IR absorbance characteristics of precipitates from bacterially oxidized iron solutions

Test material	Absorbance characteristics[a]						
	OH stretch[b]	NH stretch	H_2O deformation	NH_4 deformation	ν_3 (SO_4)		ν_3 (SO_4)
$NaFe_3(SO_4)_2(OH)_6$	(S) 3,354				1,184		1,094
$KFe_3(SO_4)_2(OH)_6$	(S) 3,383				1,180		1,083
	(P) 3,385		1,635		1,181		1,080
$(H_3O^+)Fe_3(SO_4)_2(OH)_6$	(S) 3,358		1,635		1,198		1,088
	(P) 3,365	3,330	1,632		1,190		1,085
$(NH_4)Fe_3(SO_4)_2(OH)_6$	(S) 3,408	3,200	1,630	1,423	1,193		1,076
		Jarositic precipitates					
Resting cell oxidation							
0.5 M $FeSO_4$, 0.5 M Na_2SO_4	3,359s		1,639s		1,180b		1,089s
0.5 M $FeSO_4$, 0.5 M K_2SO_4	3,378s		1,624s		1,185b		1,080s
0.2 M $FeSO_4$, 0.5 M $(NH_4)_2SO_4$	3,395	3,200sh	1,624	1,416	1,182b 1159		1,070s
0.2 M $FeSO_4$, 0.2 M $NaClO_4$	3,290sp				1,180sh		1,078s
0.2 M $FeSO_4$, 0.2 M $NaClO_4$ 0.2 M Li_2SO_4	3,347sp		1,636w		1,184		1,086s
Cell-free filtrates (0.2 M)							
+ Solid Na_2SO_4	3,347sp		1,637		1,182		1,089s
+ Solid $(NH_4)_2SO_4$	3,380	3,250sh	1,605	1,410	1,190		1,070s
+ Solid RbCl	3,375s		1,621		1,189b		1,076b,s
		Amorphous precipitates					
Resting cell oxidation							
0.5 M $FeSO_4$	3,270b		1,624		1,170sh	1,110s	1,092
0.2 M $FeSO_4$	3,318b		1,629		1,175sh	1,118s 1,115s	1,100
0.16 M $FeSO_4$, 0.2 M $MgSO_4$	3,360b		1,604		1,180sh	1,105	1,085
0.2 M $FeSO_4$, 0.2 M Li_2SO_4	3,330b		1,630		1,176sh	1,115s	1,074
Cell-free filtrates							
No additions	3,300b		1,626			1,112s 1,120s	1,070sh
+ 0.2 M Na_2SO_4 (solid)	3,380b		1,630		1,177sh	1,111 1,147s	1,085
+0.33 M Na_2SO_4 (solution)	3,300b		1,627		1,198	1,110	1,094
+ 0.2 M NaCl (solid)	3,360b		1,624		1,167	1,119s	1,102
+ 0.2 M $NaNO_3$ (solid)	3,365b		1,623		1,181	1,110s	1,085
+ 0.2 M Li_2SO_4 (solid)	3,330b		1,619		1,178sh	1,123s 1,128s	1,079
+ 0.2 M $MgSO_4$ (solid)	3,300b		1,623		1,190w	1,110	
+ 0.1 M NH_4Cl (solid)	3,340b	3,200sh	1,622	1,412w	1,150	1,115s	1,088

[a] b, Broad; s, strong; sh, shoulder; sp, sharp; w, weak.
[b] Data from (S) Shokarev et al. (19) or (P) Powers et al. (17).
[c] Data from Margulis et al. (12).

lent cations and increased sulfate concentrations did not lead to jarosite formation after abiotic oxidation, nor did bacterial oxidation produce jarosite unless both ionic requirements were met. The latter was demonstrated by bacterially filtering $FeSO_4$ solutions that had been oxidized by *T. ferrooxidans* before complete precipitation. When $FeSO_4$ alone was present at pH 2.5, the solutions ultimately deposited the amorphous type of precipitate. However, if solid

TABLE 3—*Continued*

Absorbance characteristics[a]									
δ (OH)	ν_1 (SO_4)		ν_4 (SO_4)	ν_4 (SO_4)	Coordinated H_2O[c]	τ (OH)	τ (OH)	ν_2 (SO_4)	τ (SO_4)
1,025	1,008			629		510	478	445	346
1,012	1,003			628		509	474	446	336
1,003			650sh	626		505	469	441	335
1,010	1,006			623		510	472	450	346
1,002			650sh	616		505	465	440	341
1,000	997			626		507	469		338
Jarositic precipitates									
1,017s	1,000		650sh	621	565w	509	475	440sh	
1,014s	995		645sh	620	570w	500	465 480	440	
1,004s	984			620	570w	495	460		
1,009s	992			620sh		493	469	440	
1,010s	998			622		497	473	440sh	
1,017s	1,003			622sp	570	502	471	440	350
1,001s	982			620	568	487 510	465	440	
1,006b,s	975			619	570w	492	470		
Amorphous precipitates									
1,050	969	695b	650		570				
1,043	978	689	644		570				
1,042	970	690	645						
	989								
1,039	973	692	650		570				
1,043sh	972	693	652		570w				
1,056									
1,024	985sh	692	650	620w	570				
1,040	975	690	650w,sh		570				
1,040sh	973	692	650		572				
1,042	974	686	651		570				
1,050	970	697	651w		570				
1,057	970	697	649		575				
1,054	978	697b	650w		570w				

Na_2SO_4, K_2SO_4, or $(NH_4)_2SO_4$ was added before precipitation in the absence of bacteria, jarositic precipitates formed on standing. The addition of the solid chlorides or nitrates of NH_4^+ or Na^+ yielded amorphous precipitates, as did the addition of concentrated salt solutions, including solutions of the sulfates that produced jarosites, when added as solid salts (Table 3).

The requirement for excess sulfate during jarosite formation in bacterially oxidized filtrates was most pronounced when sodium was

supplied as the monovalent cation, but this requirement was progressively less stringent for NH_4^+, K^+, and Rb^+. In the last instance, jarosite formation occurred even if RbCl was used, although the yield was enhanced by simultaneous introduction of SO_4^{2-} as Li_2SO_4 or $MgSO_4$. In those cases, flame photometric and atomic absorbance analyses showed that neither Li^+ or Mg^{2+} was incorporated in the jarosites produced.

Hydronium jarosite was produced from the sterile filtrates of bacterially oxidized $FeSO_4$ solutions if the pH was brought to 2.3 to 2.4 and sulfate levels were maintained in excess. This could be accomplished either by the addition of the solid sulfates of cations unsuitable for jaro-

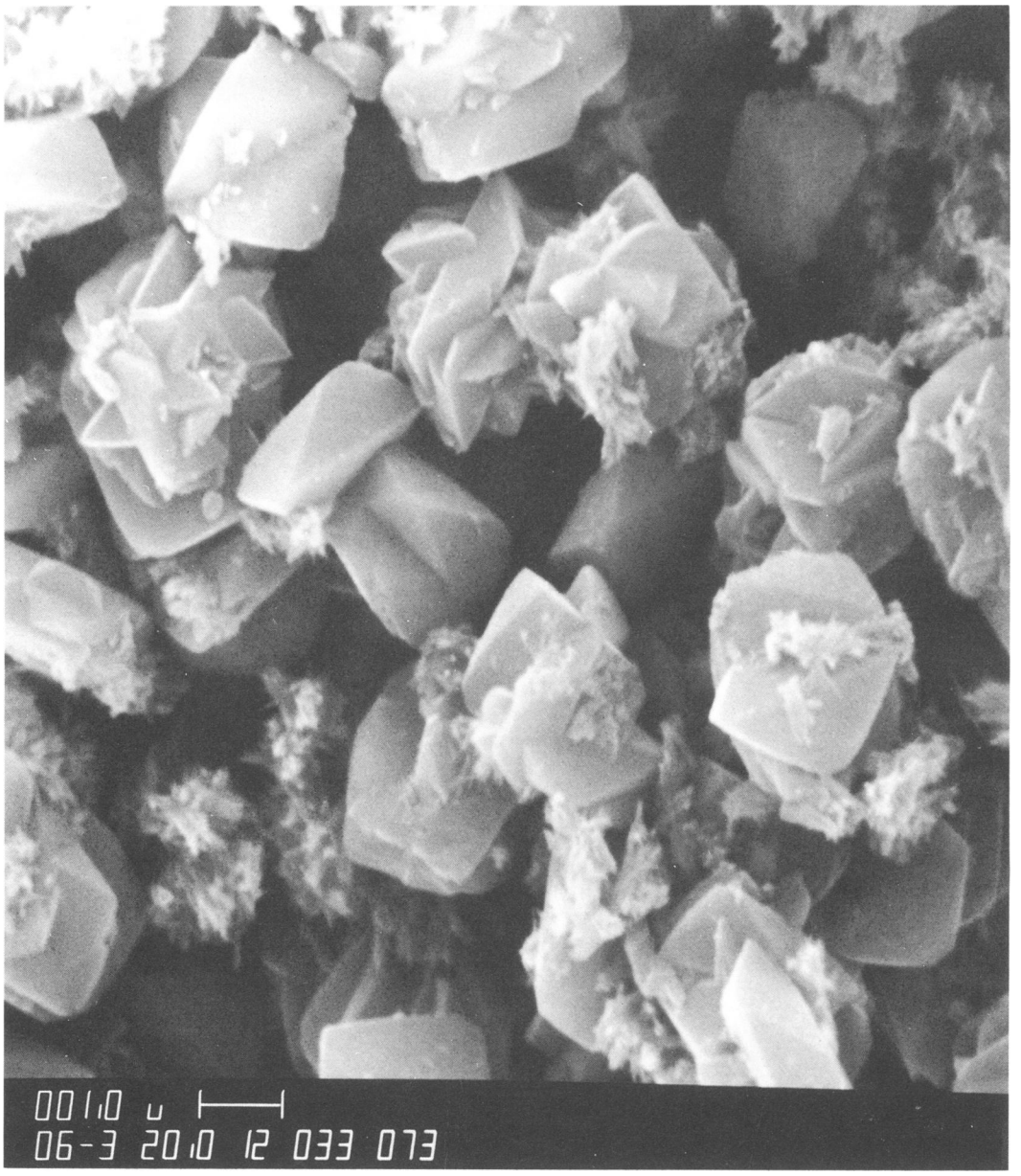

FIG. 2. Scanning electron micrograph of crystalline ammonio jarosite with stringy adherent amorphous ferric hydroxysulfate.

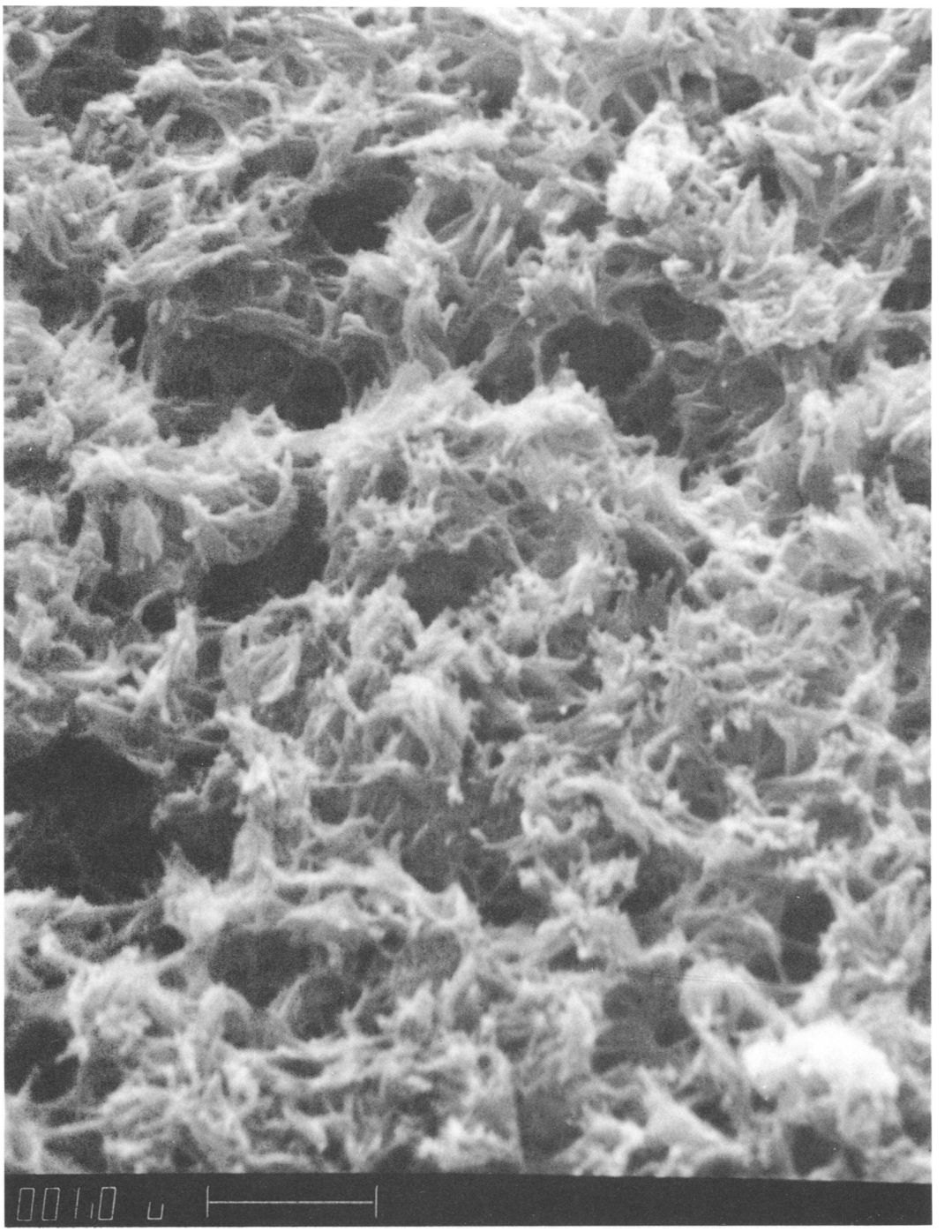

FIG. 3. Scanning electron micrograph of amorphous ferric hydroxysulfate showing its fibroporous microstructure.

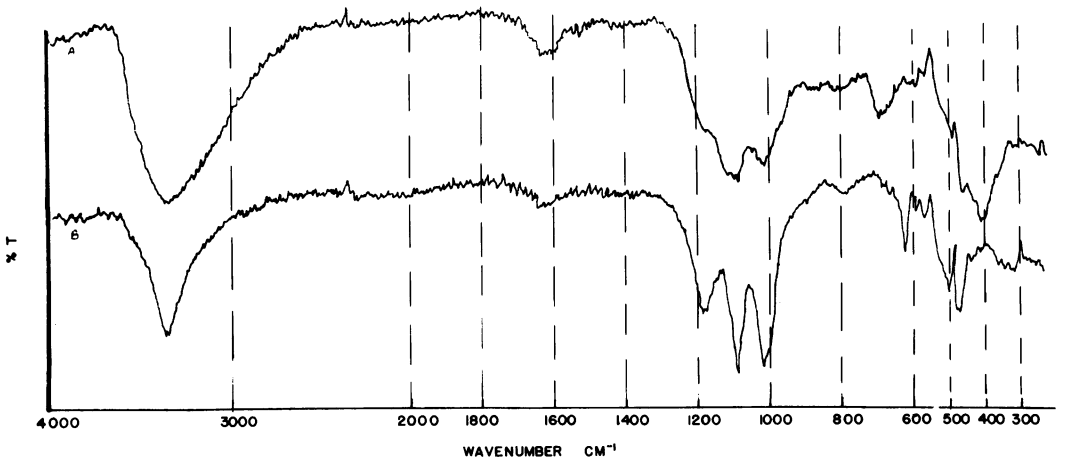

FIG. 4. Purification of natrojarosite by washing with 4N HCl. (A) Compound IR spectrum of mixture of amorphous ferric hydroxysulfate and natrojarosite, formed from bacterially oxidized 0.2 M $FeSO_4$ by addition of solid Na_2SO_4 to a final concentration of 0.2 M. (B) IR spectrum of natrojarosite, obtained from (A) after washing successively with 4 N HCl, pH 2.5 H_2SO_4, water, and acetone and then drying at 80°C in a forced draft oven.

site formation (i.e., Li^+, Mg^+, or $CH_3NH_3^+$) or by using partially oxidized $FeSO_4$ solutions of high molarity to provide increased ratios of sulfate to ferric ions when oxidation was initiated.

DISCUSSION

To assess the role of sulfate in the oxidation and precipitation of iron by *T. ferrooxidans*, it should be recognized that, after hydrolysis takes place, the ferric ions formed in solution are complexed by sulfate and hydroxide anions as well as water molecules. Since several possibilities exist for the formation of hydroxo and sulfato complexes of Fe(III), it is in itself interesting that only certain complexes form. The nature of Fe(III) complex formation in aqueous solution affects the free energy of iron oxidation and therefore relates to the physiological mechanism of chemolithotrophic iron oxidation (4).

The investigations reported by Ivarson and co-workers (7) emphasized the formation of jarosites in acid ferrous sulfate solutions oxidized by growing cells of *T. ferrooxidans*. Since the solutions that they used contained excess sulfate and the monovalent cations required for jarosite formation, it is not surprising that those authors made scant reference to the precipitation of other Fe(III) products by bacterially oxidized iron solutions.

In jarosites, octahedral ferric ions are bridged by coordinated OH^- and SO_4^{2-} anions (17) in the manner shown in Fig. 9. Margulis et al. (12) found that the jarositic complex formed slowly and incompletely in a range of pH 1.8 to 2.7 at 22°C when KOH was added to acid solutions of $Fe_2(SO_4)_3$. The precipitation of jarosite was more rapid and complete as the temperature was increased. Accompanying the jarosite, particularly at the lower temperatures, was a substance characterized by the authors as a colloidal basic sulfate of composition $2Fe_2O_3 \cdot SO_3 \cdot xH_2O$ (12, 13). By following the precipitation with time, they observed that the amorphous precipitate was eventually replaced by jarosite. This was attributed to dissolution of the substance (considered by them to be a colloidal aggregate), followed by reformation of ionic complexes which gave rise to jarosite. It is interesting to note that Ivarson et al. (7) mention an uncharacterized reddish amorphous precipitate, obtained in an attempt to produce hydronium jarosite by bacterial oxidation of an acid $FeSO_4$ solution containing Li_2SO_4, LiCl, and H_3PO_4.

Given the extreme insolubility of the jarosites in acid sulfate solutions, but their slowness to precipitate from solution as bacterial oxidation takes place, it is unlikely that the jarositic complexes are initial products of bacterial iron oxidation. This line of reasoning is supported by the observations of basic ferric sulfate precipitation mentioned above (12) as well as our finding that other products are alternative to jarosite when either abiotic or bacterial oxidation of Fe^{2+} occurs and the conditions for jarosite precipitation are not met.

Although Margulis and co-workers (12) had found in their chemical studies that the amorphous basic sulfate initially precipitated at room temperature from ferric sulfate solutions, we

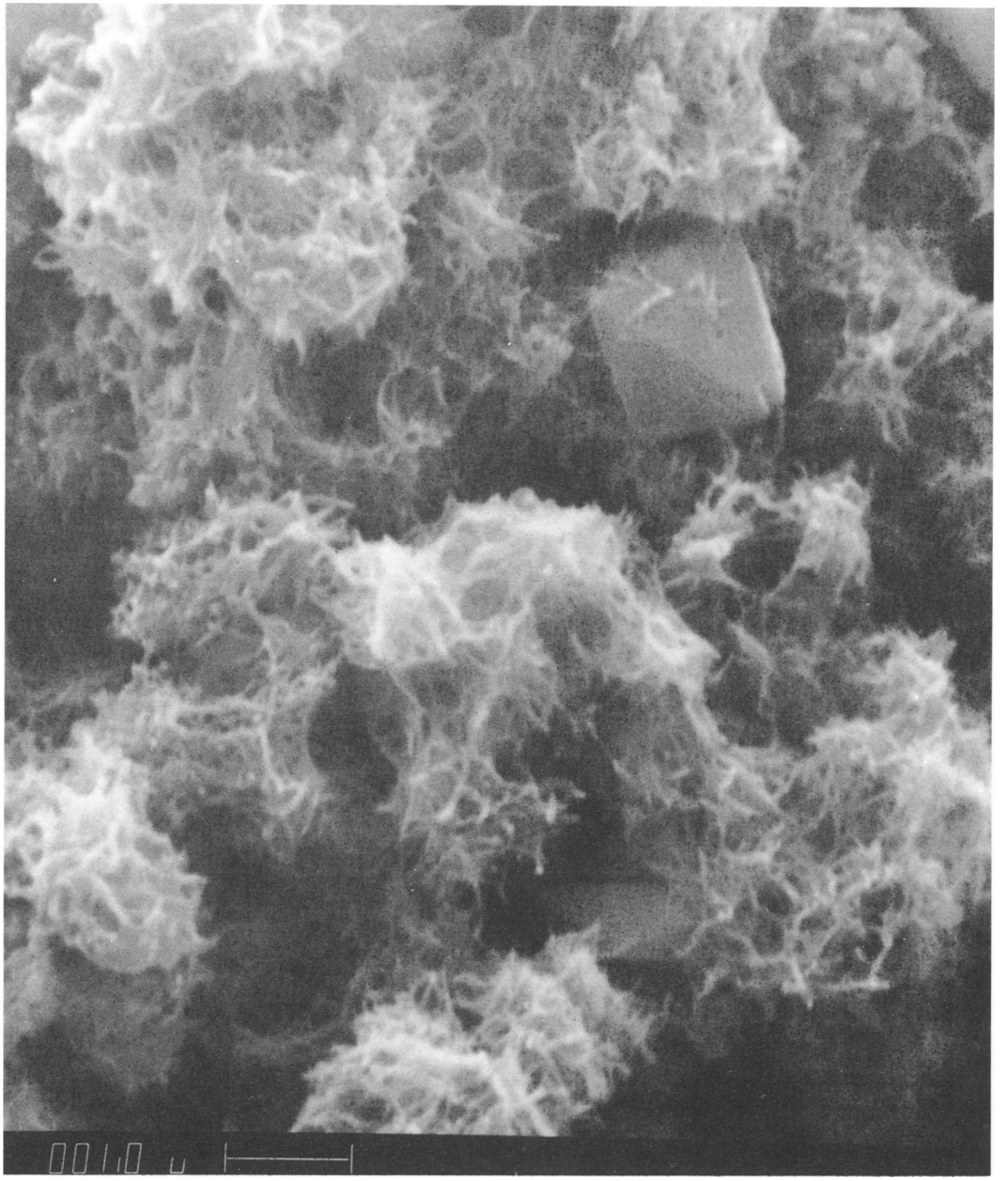

FIG. 5. Scanning electron micrograph of mixture of natrojarosite and amorphous ferric hydroxysulfate, the compound spectrum of which is shown in Fig. 4A.

observed that precipitates from abiotic oxidation of ferrous sulfate solutions, at low pH, contained some sulfate but were predominantly FeOOH in IR absorbance characteristics. Even though a more precise characterization of the precipitates by X-ray diffraction has not been carried out, we showed by IR spectra and chemical analyses that the abiotic oxidations studied did not produce the same Fe(III)-sulfato complexes as did bacterial oxidation. The sulfato complexes formed in solution by bacterial oxidation produced amorphous ferric hydroxysulfates or jarosites (or both) in a manner similar to that shown by Margulis et al. (12) for $Fe_2(SO_4)_3$ solutions plus KOH.

The bacterial jarosites form readily at the

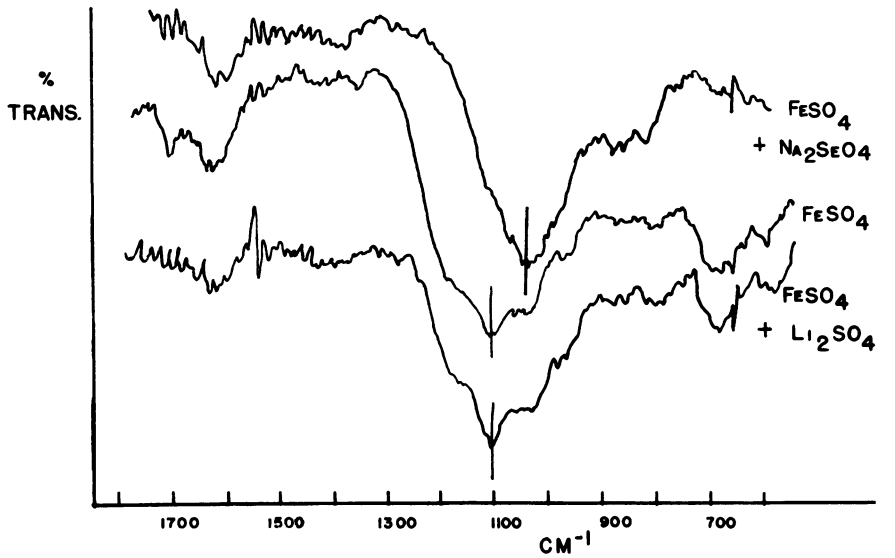

FIG. 6. Comparison of the IR spectrum of a partially selenated amorphous precipitate, formed by bacterial oxidation, with nonselenated amorphous bacterial ferric hydroxysulfate precipitates. The shift of major absorbance from $\approx$1,115 cm^{-1} in the amorphous sulfate to $\approx$1,045 cm^{-1} in the partially selenated analog is interpreted as the partial loss of sulfate activity at $\approx$1,115 cm^{-1} unmasking $\delta(OH^-)$ absorption at $\approx$1,045 cm^{-1}.

temperatures of natural environments, even if the bacteria have been removed from the system before precipitation. The complexes in solution appear to be precursors for both the amorphous product and the jarosites, since the extent to which either is produced from sterile filtrates of bacterially oxidized iron solutions depends upon the concentration of SO_4^{2-} and requisite monovalent cations. Sterile filtrates which would produce amorphous precipitates on standing form crystalline jarosites instead, if appropriate cations are added as the solid sulfates.

There is further evidence that the soluble bacterial iron oxidation products, which gave rise to amorphous and jarositic precipitates, are sulfate complexes. The UV absorption spectrum of Fe(III) with sulfate at acid pH shows a charge transfer absorption maximum at 305 nm (generally attributed to the sulfate complex [1, 25]), which changes sharply if anions such as Cl^- or ClO_4^- are added at concentrations comparable to that of SO_4^{2-}. In preliminary investigations, we found that the charge transfer absorption bands encountered in undiluted bacterially oxidized iron solutions were accompanied by long-wavelength shoulders which extended into the visible spectrum. The existence of these long-wavelength UV-absorbing complexes was further confirmed by extraction into propylene carbonate according to the technique of Itoh et al. (5). Those authors interpreted the long-wavelength absorption in extracts of ferric perchlorate solutions to be due to the presence of polymerized Fe(III)-hydroxo complexes, similar perhaps to the stable aqueous hydroxo-Fe(III) polymers prepared by Spiro and Saltman (21). In the latter instance, NO_3^- functioned as counterions balancing the net positive charges of the hydroxo complexes, a role that would be assumed by SO_4^{2-} for hydrolytic iron polymers in media supporting bacterial iron oxidation.

The postulated formation of polymeric intermediates is the basis for proposing a mechanism of bacterial ferric hydroxysulfate formation that agrees with the following experimental observations: (i) The amorphous precipitates have variable Fe^{3+}/SO_4^{2-} ratios (3.5 to 5) compared with the jarosites ($\approx$1.5). (ii) The amorphous species does not incorporate univalent cations. When these cations are found associated with well-washed amorphous precipitates, it is due to admixture of jarosite. (iii) The deposition of both amorphous and jarositic precipitates from bacterially oxidized iron solutions continues long after all bacteria have been removed from the system and oxidation has ceased. Intermediates capable of forming jarosites are present in bacterially oxidized iron solutions that deposit amorphous precipitates. Addition of the required cations with sufficient sulfate yields jarosites in those systems but not in acid sulfate solutions that have been oxidized chemically at temperatures compatible with bacterial oxidation. (iv) Jarosite formation was prevented and amor-

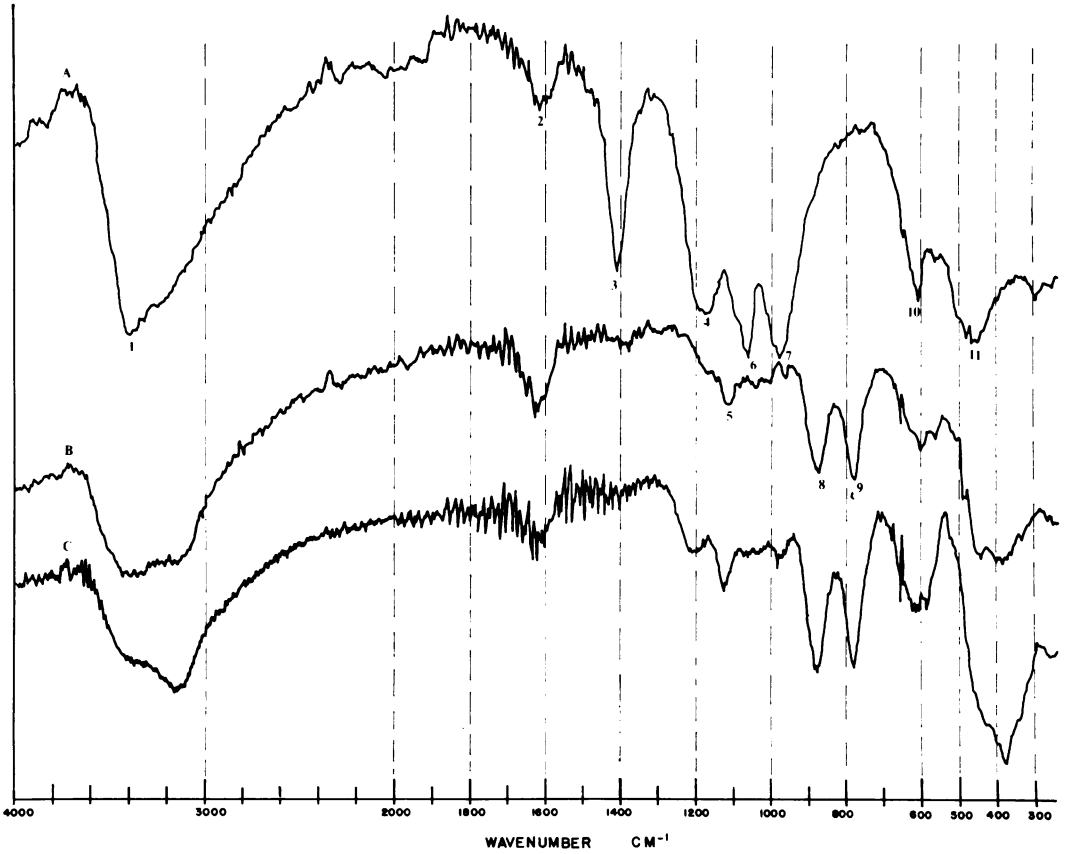

FIG. 7. Comparison of IR spectra of precipitates produced by bacterial oxidation with those formed abiotically in 0.2 M $FeSO_4$ solutions containing 0.2 M $(NH_4)_2SO_4$. (A) Bacterial oxidation at pH 2.5. (B) Oxidized spontaneously at pH 6.0. (C) Oxidized by H_2O_2 at pH 2.5. Numbers 1 through 7, 10, and 11 as in Fig. 1. 8 and 9, δ(OH) of FeOOH.

phous precipitates formed instead in bacterially oxidized iron solutions after the introduction of anions such as Cl^-, NO_3^-, or ClO_4^-. This was reversed if sufficient SO_4^{2-} was added, in a manner that did not dilute the iron complexes in solution (for example, by adding solid lithium or magnesium sulfates). Dilution of the iron sulfate complexes even with concentrated sodium sulfate solutions yielded amorphous precipitates. (v) The rate and extent of bacterial jarosite formation with different monovalent cations is related to the ionic radii of the cations, as reported by Ivarson and co-workers (7). Thus, at equivalent sulfate levels, NH_4^+ or Na^+ produced mixtures of jarosites and amorphous products, but K^+ produced a nearly pure jarosite. However, increasing the sulfate concentration by adding Li_2SO_4 to $FeSO_4$ solutions containing sodium ions yielded nearly pure sodium jarosite. (vi) IR spectra of the amorphous precipitates show that the SO_4^{2-} present approximates T_d symmetry. As interpreted by Nakamoto (14), this can be explained as due to SO_4^{2-} as ligand in the outer coordination sphere of the octahedral cation (2). The selenate analog of the amorphous basic ferric sulfate reveals the presence of bridging Fe-O-bonds that would otherwise be masked by the broad ν_3 mode of $T_d(SO_4^{2-})$. However, further information is needed to fully characterize the amorphous precipitate.

We infer that the soluble precursor of the amorphous precipitate is a hydroxo-bridged polymer which contains SO_4^{2-} in outer coordination and precipitates as the result of further polymerization and charge stabilized aggregation. The same precursor forms jarosite after incorporating additional SO_4^{2-} and linking three hydroxo-bridged iron octahedra with tridentate bridging sulfate anions. This reduces the symmetry of SO_4^{2-} from T_d to C_{3v} as shown by comparing IR spectra of SO_4^{2-} in the amorphous and jarositic precipitates. Apparently, the

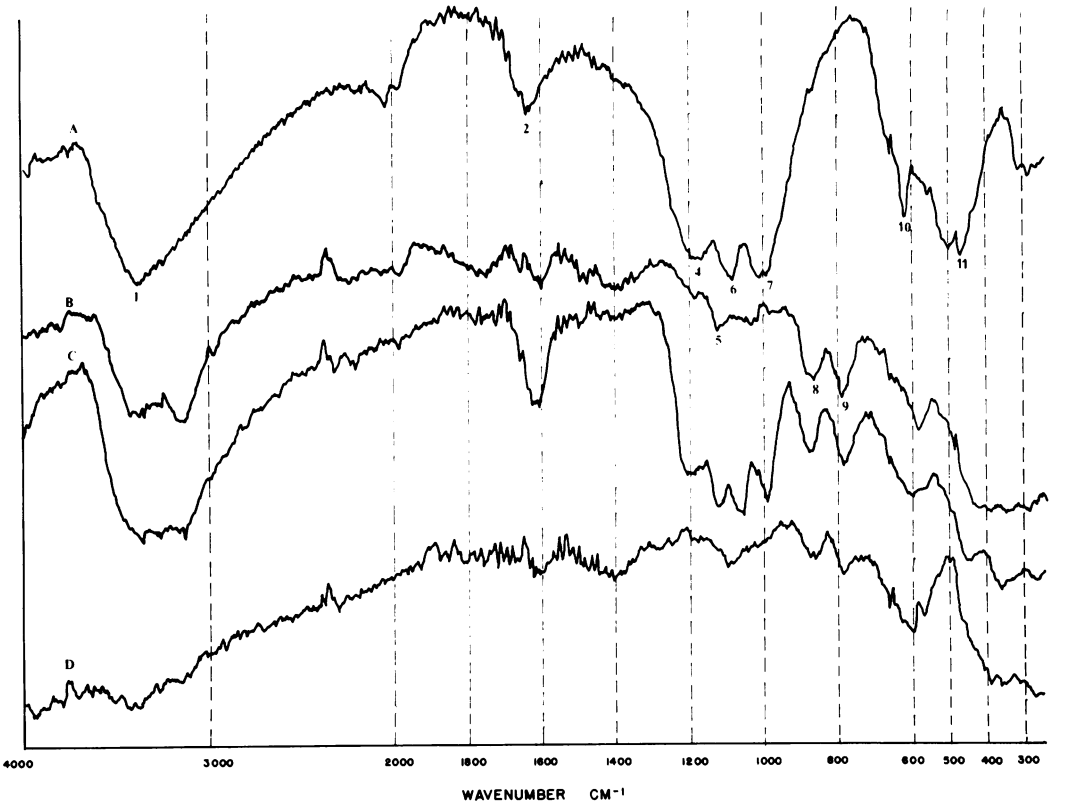

FIG. 8. Comparison of IR spectra of precipitates produced by bacterial oxidation with those formed abiotically in 0.2 M Fe_2SO_4 solutions containing 0.2 M Na_2SO_4. Spectra A, B, and C and numbers as in Fig. 7. Spectrum D, oxidized spontaneously at pH 9.0. The spectrum is essentially that of Fe_3O_4 (magnetite) (16).

introduction of SO_4^{2-} into the inner coordination sphere of Fe^{3+} and bridging of the iron octahedra requires stabilization by the monovalent cations, which connect sulfates in parallel arrays of sulfato-, hydroxo-bridged iron octahedra (Fig. 9, 10). Since this did not occur when acid ferrous sulfate solutions were chemically oxidized at room temperature, but does occur rapidly at higher temperatures from Fe(III) solu-

TABLE 4. Incorporation of monovalent cations in jarosites precipitated by resting cell oxidation of acid $FeSO_4$ solutions

Addition to 0.2 M $FeSO_4$ (pH 2.5)	% M[a] determined	% M theoretical	% of theoretical
0.1 M $(NH_4)_2SO_4$	2.3	2.9	79.3
0.25 M $(NH_4)_2SO_4$	2.3		79.3
0.5 M $(NH_4)_2SO_4$	2.6		89.7
1.0 M $(NH_4)_2SO_4$	2.6		89.7
0.25 M Na_2SO_4	4.2	4.76	88.2
	4.0		84.0
0.25 M K_2SO_4	6.4	7.8	82.1
	6.2		79.5

[a] Percentage of dry weight, Na^+, K^+, or NH_4^+.

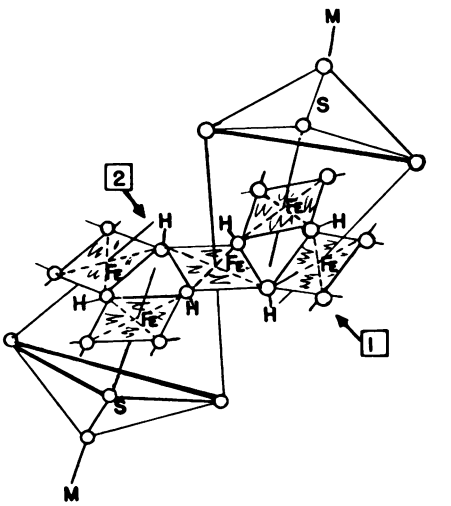

FIG. 9. Relationship of octahedral Fe^{3+} to bridging OH^- and SO_4^{2-} in jarosites. According to Powers et al. (17), the presence of coordinated water in jarosites may be explained by nonbridged sites between iron octahedra (i.e., site 1 occupied by water molecules) rather than OH^- shown at site 2. S, Sulfur; Fe, Fe^{3+}; M, univalent cation.

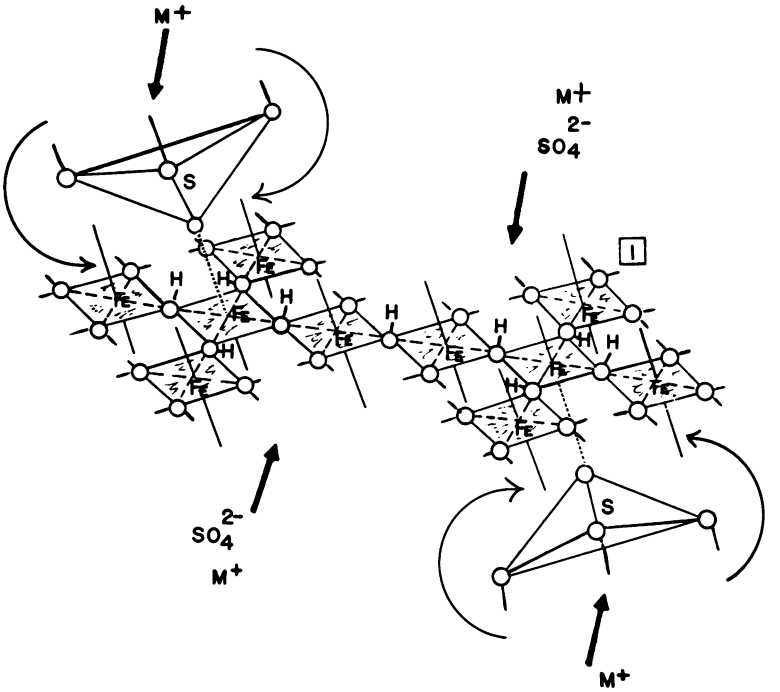

FIG. 10. Postulated relationship of octahedral Fe^{3+} to OH^- and SO_4^{2-} in a proposed polymeric precursor of jarosites and amorphous ferric hydroxysulfates. The incorporation of appropriate monovalent cations (M^+) and SO_4^{2-} leads to bridging of the Fe^{3+} octahedra by covalently bonded OH^- and SO_4^{2-} to produce the jarositic structure shown in Fig. 9. Alternatively, further polymerization and aggregation of the precursor yields amorphous ferric hydroxysulfate precipitation. Tetrahedral SO_4^{2-} is shown connected to Fe by a dotted line to indicate that it may be in the outer coordination sphere (2), as in the amorphous precipitate, and that there may be water molecules at inner coordination sites between the Fe^{3+} and SO_4^{2-}. This would account for more coordinated water in the amorphous precipitate and the polymeric precursor than in jarosite due to less extensive bridging of the iron octahedra in the first two instances.

tions (13), it might be reasoned that the bacterial process catalyzes the production of ferric hydroxysulfate polymers from specific iron hydroxo-sulfato complex intermediates by lowering the activation energy for their formation. Then, depending upon the ionic environment, the iron complex precipitates by forming either amorphous ferric hydroxysulfates or crystalline jarosites.

ACKNOWLEDGMENTS

This work was partly supported by contract EF-77-G-01-2749 from the Department of Energy.

We gratefully acknowledge information concerning I.R. spectroscopy of ferric hydroxysulfates supplied by George R. Rossman, Division of Geological and Planetary Sciences, California Institute of Technology. We also express appreciation for atomic absorption analysis by Max Budd, Department of Geological Sciences, State University of New York, Binghamton; for scanning electron microscopy by Linda Melanson, Department of Biological Sciences, State University of New York, Binghamton; and for the technical assistance in ferric hydroxysulfate preparation and analysis by Nick Santoro, Department of Biological Sciences, State University of New York, Binghamton.

LITERATURE CITED

1. **Bastian, R., R. Weberling, and F. Palilla.** 1953. Spectrophotometric determination of iron as ferric sulfate complex. An ultraviolet study. Anal. Chem. **25**:284–288.
2. **Bjerrum, J.** 1967. Coordination in the second sphere, p. 178–186. *In* G. B. Kaufman (symposium chairman), Werner centennial. American Chemical Society. Washington, D.C.
3. **Duncan, D. W., and A. Bruynsteyn.** 1971. Enhancing bacterial activity in a uranium mine. Can. Min. Metall. Bull. **64**:32–36.
4. **Ingledew, W. K., J. C. Cox, and P. J. Halling.** 1977. A proposed mechanism for energy conservation during Fe^{2+} oxidation by *Thiobacillus ferrooxidans*: chemiosmotic coupling to net H^+ influx. FEMS Microbiol. Lett. **2**:193–197.
5. **Itoh, H., M. Katsuo, and S. Ikeda.** 1973. Extraction of iron (III) from perchlorate solutions into propylene carbonate. J. Inorg. Nucl. Chem. **35**:3632–3636.
6. **Ivarson, K. C.** 1973. Microbiological formation of basic ferric sulfates. Can. J. Soil Sci. **53**:315–323.
7. **Ivarson, K. C., G. J. Ross, and N. M. Miles.** 1979. The microbiological formation of basic ferric sulphates: II. Crystallization in presence of potassium, ammonium, and sodium salts. Soil Sci. Soc. Am. J. **43**:908–912.
8. **Johnson, M. J.** 1941. Isolation and properties of a pure yeast polypeptidase. J. Biol. Chem **137**:575–586.
9. **Lazaroff, N.** 1963. Sulfate requirement for iron oxidation by *Thiobacillus ferrooxidans*. J. Bacteriol. **85**:78–83.

10. **Lazaroff, N.** 1977. The specificity of the anionic requirement for iron oxidation by *Thiobacillus ferrooxidans*. J. Gen. Microbiol. **101**:85–91.
11. **Leathen, W. W., S. A. Braley, and L. D. McIntyre.** 1953. The role of bacteria in the formation of acid from certain sulfuritic constituents associated with bituminous coal. II. Ferrous iron oxidizing bacteria. Appl. Microbiol. **1**:65–68.
12. **Margulis, E. V., L. S. Getskin, N. A. Zapuskalova, and L. I. Beisekeeva.** 1976. Hydrolytic precipitation of iron in the $Fe_2(SO_4)_3$-KOH-H_2O system. Russ. J. Inorg. Chem. **21**:996–999.
13. **Margulis, E. V., L. A. Savchenko, M. M. Shokarev, L. I. Beisekeeva, and F. I. Vershinina.** 1975. The amorphous basic sulphate $2Fe_2O_3 \cdot SO_3 \cdot H_2O$. Russ. J. Inorg. Chem. **20**:1045–1048.
14. **Nakamoto, K.** 1967. Recent infrared studies on Werner complexes, p. 396–407. *In* G. B. Kaufman (symposium chairman), Werner centennial. American Chemical Society, Washington, D.C.
15. **Nakamoto, K.** 1978. Infrared and Raman spectra of inorganic and coordination compounds, third ed. John Wiley & Sons, New York.
16. **Nyquist, R. A., and R. O. Kagel.** 1971. Infrared spectra of inorganic compounds. Academic Press, Inc., New York.
17. **Powers, D. A., G. R. Rossman, H. H. Schugar, and H. B. Gray.** 1975. Magnetic behavior and infrared spectra of jarosite, basic iron sulfates and their chromium analogs. J. Solid State Chem. **13**:1–13.
18. **Schnaitman, C. A., M. S. Korczynski, and D. G. Lundgren.** 1969. Kinetic studies of iron oxidation by whole cells of *Ferrobacillus ferrooxidans*. J. Bacteriol. **99**:552–557.
19. **Shokarev, M. M., E. V. Margulis, F. I. Vershinina, L. I. Beisekeeva, and L. A. Savchenko.** 1972. Infrared spectra of iron (III) hydroxide sulphates and hydroxides. Russ. J. Inorg. Chem. **17**:1293–1296.
20. **Silverman, M. P., and D. G. Lundgren.** 1959. Studies on the chemoautotrophic iron bacterium *Ferrobacillus ferrooxidans*. I. An improved medium and harvesting procedure for securing high cell yields. J. Bacteriol. **77**:642–647.
21. **Spiro, T. G., and P. Saltman.** 1974. Inorganic chemistry, IV. Biopolymerization, p. 14–15. *In* A. Jacobs and M. Worwood (ed.), Iron in biochemistry and medicine. Academic Press, Inc., London.
22. **Steiner, M., and N. Lazaroff.** 1974. Direct method for continuous determination of iron oxidation by autotrophic bacteria. Appl. Microbiol. **28**:872–880.
23. **Tuovinen, O. H., and L. Carlson.** 1979. Jarosite in cultures of iron-oxidizing *Thiobacilli*. Geomicrobiol. J. **1**:205–210.
24. **Tuovinen, O. H., S. I. Niemela, and H. G. Gyllenberg.** 1971. Effect of mineral nutrients and organic substances on the development of *Thiobacillus ferrooxidans*. Biotechnol. Bioeng. **13**:517–527.
25. **Whiteker, R. A., and N. Davidson.** 1953. Iron-exchange and spectrophotometric investigation of iron (III) sulfate complex ions. J. Am. Chem. Soc. **75**:3081–3085.